Low-Cost Circularly Polarized Origami Antenna

Syed Imran Hussain Shah, *Student Member, IEEE*, Manos M. Tentzeris, *Fellow, IEEE*, and Sungjoon Lim, *Member, IEEE*

***Abstract*—In this letter, we present a novel circularly polarized (CP) origami antenna. We fold paper in the form of an origami tetrahedron to serve as the substrate of the antenna. The antenna comprises two triangular monopole elements that are perpendicular to each other. Circular polarization characteristics are achieved by exciting both elements with equal magnitudes and with a phase difference of 90°. In this letter, we explain the origami folding steps in detail. We also verify the proposed concept of the CP origami antenna by performing simulations and measurements using a fabricated prototype. The antenna exhibits a 10-dB impedance bandwidth of 70.2% (2.4–5 GHz), and a 3-dB axial-ratio bandwidth of 8% (3.415–3.7 GHz). The measured left-hand circular polarization gain of the antenna is in the range of 5.2–5.7 dBi for the 3-dB axial-ratio bandwidth.**

***Index Terms*—Circular polarization, origami antenna, paper-based antenna, tetrahedron.**

I. Introduction

CIRCULARLY polarized (CP) antennas play an important role in various modern wireless communication technologies. Compared to the linearly polarized (LP) antennas, CP antennas reduce the polarization loss, multipath reflection, and other kinds of interferences [1]. In literature, numerous techniques have been proposed to design CP antennas. In [2], directional CP characteristics were achieved by employing a four-feed network and four sequentially rotated inverted-F antennas (IFAs). In [3], a directional CP logarithmic spiral antenna was presented using reflectors and directors. In [4], an LP antenna was converted to a CP antenna by placing it at a certain distance from a metasurface. CP operation was achieved by employing two eight-mode substrate-integrated waveguide antennas that were orthogonal to each other [5].

Origami is a Japanese term meaning "folding paper." Various shapes can be easily adopted using origami techniques, and this can present significant advantages in electromagnetic applications. For instance, in [6] and [7], frequency-reconfigurable origami antennas were presented.

Manuscript received September 23, 2016; revised February 27, 2017; accepted April 10, 2017. Date of publication April 13, 2017; date of current version July 24, 2017. This work was supported in part by the Chung-Ang University Research Grants in 2015 and in part by the Ministry of Science, ICT, and Future Planning, Korea, under the Information Technology Research Center support program IITP-2017-2012-0-00559 supervised by the Institute for Information & Communications Technology Promotion. *(Corresponding authors: Manos M. Tentzeris; Sungjoon Lim.)*

S. I. H. Shah and S. Lim are with the School of Electrical and Electronics Engineering, College of Engineering, Chung-Ang University, Seoul 06974, South Korea (e-mail: engr.shahsyedimran@gmail.com; sungjoon@cau.ac.kr).

M. M. Tentzeris is with the School of Electrical and Computer Engineering, College of Engineering, Georgia Institute of Technology, Atlanta, GA 30332 USA (e-mail: etentze@ece.gatech.edu).

Color versions of one or more of the figures in this letter are available online at http://ieeexplore.ieee.org.

Digital Object Identifier 10.1109/LAWP.2017.2694138

Compared to the conventional printed circuit board (PCB)-based antennas [8], [9], the paper-based origami antenna has many benefits for military applications requiring mobility as well as fast and easy deployment. Therefore, in the present study, we propose a CP tetrahedral origami antenna with tilted beam for military applications. For instance, when the antenna is not used, a soldier carries a few sheets of papers. When the antenna is used, a soldier can quickly build the antenna using origami. In addition, a tilted beam CP antenna can be used for ground-to-air communication such as unmanned aerial vehicle and for 5G communications [10]. We fold paper into an origami tetrahedron to realize the substrate of the antenna. In order to have a tilted beam, a triangular monopole is designed on the corner reflector of the tetrahedron. Two triangular monopole elements are orthogonal to each other. We achieve the CP operation of the antenna by exciting both these elements with a phase difference of 90°. We build the proposed antenna on a paper substrate, which makes it a low-cost antenna. The fabrication of the antenna is quite simple and fast, as it can be realized by just folding paper. The proposed CP origami antenna has a measured 10-dB impedance bandwidth of 70.2% covering the frequency range of 2.4–5 GHz, a 3-dB axial-ratio (AR) bandwidth of 8% (3.415–3.7 GHz), and a left-hand circular polarization (LHCP) gain in the range of 5.2–5.7 dBi within the 3-dB circular AR bandwidth.

II. CP Origami Antenna Design

To verify the proposed concept, we designed a CP origami antenna, which consists of two triangular monopole elements orthogonal to each other. To excite both these elements with an equal magnitude and with a phase difference of 90°, a 1:1 T-junction divider was realized. One arm of the T-junction divider was a quarter-wavelength ($\lambda/4$) longer at central frequency of 3.5 GHz, to attain the required phase difference of 90°. In addition, we employed a $\lambda/4$ impedance transformer between port of both antennas and the T-junction to match the 50-Ω input port to two 50-Ω output ports. We used the impedance transformer to achieve better matching and to increase the width of the feeding network; this enabled us to simplify its realization (cutting copper tape films). We realized all conducting parts of the antenna using copper film tapes.

To make the antenna design simple and reproducible, we divide the antenna design procedure into three steps. First, we use four square sheets of sketching paper without any coating, with the same area (270×270 mm^2) and thickness of 0.25 mm as the substrate of the antenna. These paper sheets are labeled P-1, P-2, P-3, and P-4, as shown in Fig. 2(a).

In the first step, we realize two identical triangular monopole elements that are orthogonal to each other on sheet P-1; this enables us to satisfy one of the conditions for the CP operation. The dimensions of the three sides of the triangular monopole are $L_1 = 30$ mm, $L_2 = 30$ mm, and $L_3 = 18.17$ mm. On the

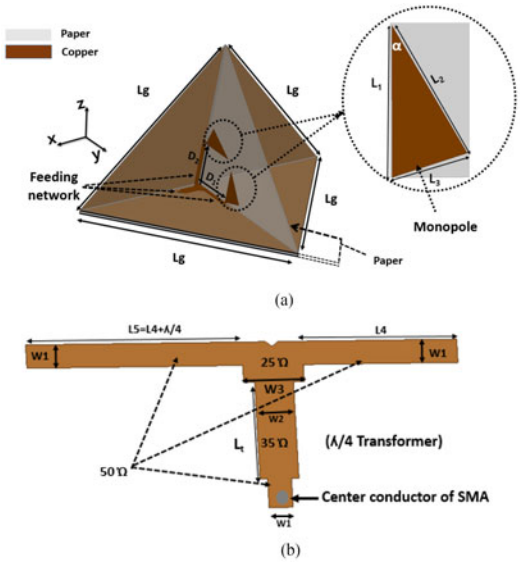

Fig. 1. (a) Geometry of CP origami antenna, $L_1 = 30$, $L_2 = 30$, $L_3 = 18.17$, $D_1 = 36.5$, $D_2 = 38.5$, $Lg = 190$. (b) Feeding network, $L_4 = 26$, $L_t = 17$, $W_1 = 4$, $W_2 = 6.58$, $W_3 = 10.3$ (units: millimeters).

second sheet, we realize a feeding network consisting of a 1:1 T-junction divider and an impedance transformer. The length of one arm of the T-junction divider (L_4) is 26.17 mm, while that of the other arm (L_5) is 43 mm (longer than L_4 by λ /4). The width (W_1) of both arms is 4 mm. The dimensions of the impedance transformer are $L_t = 17$ mm and $W_2 = 6.58$ mm. We also attach copper films of orthogonal triangle shape with dimensions of 135 mm $\times$ 135 mm $\times$ 190 mm on the top-left and top-right triangular sections of the sheets P-2 and P-3, which function as the ground parts of the two antenna elements utilized in this design. Triangular grounds of P-2 and P-3 are required because tetrahedron of Fig. 1(a) has four triangular ground sections.

In the second step, we fold appropriately all four sheets (P-1, P-2, P-3, and P-4) to realize the proposed origami CP antenna. To simplify the design process and make it repeatable, we divide the folding process into several steps. We follow similar folding procedure for all sheets; hence, here, we present only the folding steps for sheet P-1 in detail. We label the points on the edges of P-1 using the letters A, A′, B, B′, C, C′, D, and D′, the center point using O. AA′ and BB′ are the horizontal and vertical median lines, and CC′ and DD′ are the diagonals.

In step 2(a), we fold and unfold P-1 along AA′ to create a crease that divides the paper into halves [as shown in Fig. 2(b)]. In step 2(b), we fold and unfold along BB′ to add a second crease that divides the paper into quarters. Folding along CC′ and DD′ creates additional creases that divide the paper into eight triangular sections, as shown in Fig. 2(d). By folding A and A′ toward B and B′, P-1 attains the shape of a star with four pockets, as presented in Fig. 2(e).

The four pockets are indicated as 1-N (north), 1-S (south), 1-E (east), and 1-W (west), as shown in Fig. 2(f). Steps 2(a–d) are repeated for sheets P-2, P-3, and P-4 to realize three additional stars, i.e., #2, #3, and #4, as shown in Fig. 2(g)–(i).

At the end of the second step, we have four stars that are labeled as star #1, star #2, star #3, and star #4, from sheets P-1, P-2, P-3, and P-4, respectively. In the third step, stars #1, #2, #3, and #4 are joined and glued. In step 3(a), star #1 and star #4

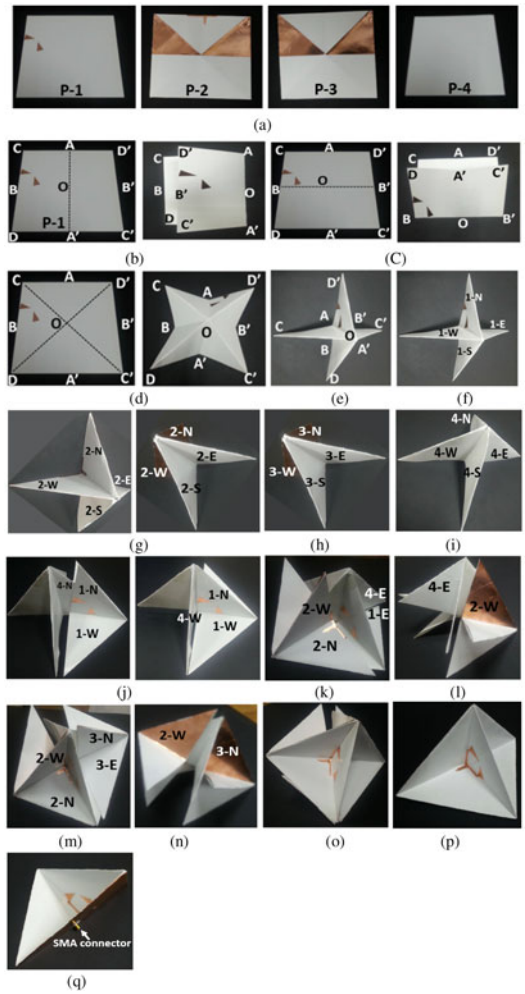

Fig. 2. Antenna design steps of the monopoles along with the feeding/matching network on four sheets of paper (a) Step 1: Selection of four paper sheets and realization of monopole, feeding network, and grounding, on three sheets of paper. (b) Step 2a: Folding and unfolding along AA′. (c) Step 2b: Folding and unfolding along BB′. (d) Step 2c: Folding and unfolding along CC′ and DD′. (e) Step 2d: Folding to form a complete star. (f) Star #l with pockets labeled as 1-N, 1-S, 1-E, and 1-W. (g) Star #2 front view and back view. (h) Star #3 back view. (i) Star #4. (j) Step 3a: Joining stars #1 and #4. (k) Step 3b: Joining star #2 (front view). (l) Joining star #2 (back view). (m). Step 3c: Joining star #3 (front view). (n) Joining star #3 (back view). (o) After joining star #3. (p) Antenna prototype top view. (q) Antenna prototype side view.

are joined together. One pocket of star #4 (4-N) is placed inside the pocket 1-N of star #1, onto which two orthogonal triangular monopole elements are realized, as shown in Fig. 2(j).

In step 3(b), star #2 is joined with stars #1 and #4, as shown in Fig. 2(k).

The 1-W pocket of star #1 and the 4-W pocket of star #4 are placed inside the pockets 2-N and 2-W of star #2, respectively; thereby, the feeding network is realized. In step 3(c), star #3 is joined to the stars #1, #2, and #4, which have already been joined together. The 1-E pocket of star #1 and the 4-E pocket of star #4 are placed inside the 3-E and 3-N pockets of star #3, respectively, as shown in Fig. 2(m)–(n). At the end of these steps, we have an origami tetrahedron structure, as presented in Fig. 2(o).

We complete our antenna design by cutting off the unnecessary parts of the paper from Fig. 2(o) that could be

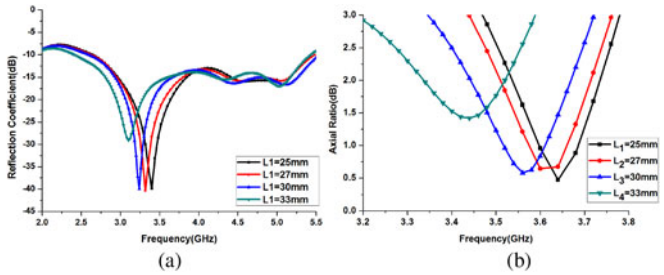

Fig. 3. (a) Simulated reflection coefficients for different L_1. (b) Simulated ARs for different L_1.

effectively utilized for the extension of the proposed topology to an array configuration. The side and top views of the final antenna prototype are displayed in Fig. 2(p)–(q). To characterize its performance, we mounted a subminiature-version-A (SMA) connector at the input port of the feeding network of the antenna topology. The signal line (center conductor of SMA) is connected to the T-junction divider, as shown in Fig. 1(b). The outer conductor of the SMA is connected to the ground plane, as shown in Fig. 2(q).

We used an ANSYS High-Frequency Structure Simulator for the design and simulation process. The dielectric constant and dielectric loss tangent of paper are considered 3.2 and 0.06, respectively [6]. The antenna is designed around a center frequency of 3.5 GHz. In order to have maximum beam direction toward 70° with the corner reflector in the tetrahedron, the triangular-shape monopole antenna is designed. The physical size of the proposed antenna is $270 \times 135 \times 135$ mm^3 and the electrical size of antenna is $1.8\ \lambda_o \times 0.9\ \lambda_o \times 0.9\ \lambda_o$ at 2 GHz. When the antenna is folded, the size becomes compact as $70 \times 70 \times 16$ mm^3. Fig. 3 shows the results of the parametric analysis to determine the optimal dimensions of the proposed antenna. For different frequencies, we could realize CP characteristics by simply tuning the length L_1 of the triangular monopole, as shown in Fig. 3(b). We plotted the reflection coefficient values and ARs by varying L_1 from 25 to 33 mm, while L_3 is fixed at 17-mm frequencies. For all these values, the 10-dB impedance bandwidth remained almost constant with a minor variation in the radiation pattern. In the present study, we set L_1 as 30 mm to obtain CP operation at around 3.5 GHz. To visualize the CP operation, in Fig. 4, we present the simulated electric-current distributions of the proposed antenna at 3.5 GHz for $t = 0$, $t = T/4$, $2T/4$, and $3T/4$, where T is the period. J_{sum1} and J_{sum2} are the vector sums of all major current components on the vertically and horizontally realized monopole elements, respectively. The vertically and horizontally realized monopole elements produce vertical LP and horizontal LP signals, which in turn generate CP signals [10].

The vector J_{total} is the resultant of the currents J_{sum1} and J_{sum2}. The vector sum J_{total} at $t = 0$ is orthogonal to that at $t = T/4$, and it rotates in a clockwise direction with time, thereby producing LHCP radiations.

III. Measurement Results

After optimizing all parameters, we fabricated an antenna prototype on a paper substrate with the thickness of 0.25 mm, in an origami tetrahedron shape, as shown in Fig. 2(p)–(q). We measured the reflection coefficient values of the proposed antenna using an Anritsu vector network analyzer (MS2038C), and

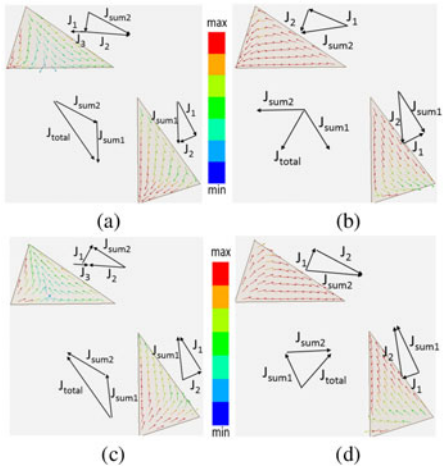

Fig. 4. Simulated electric currents in the two perpendicularly placed triangular monopole elements with period T at 3.5 GHz. (a) $t = 0$, (b) $t = T/4$, (c) $t = 2T/4$, and (d) $t = 3T/4$.

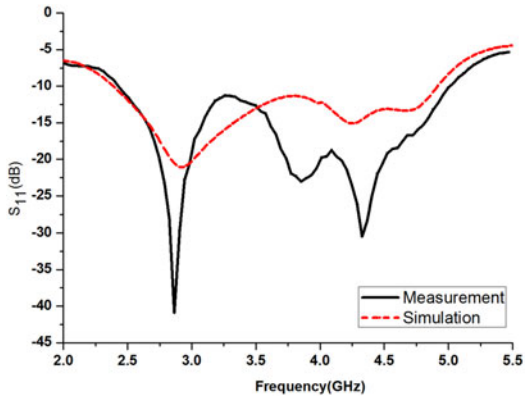

Fig. 5. Simulated and measured reflection coefficients of the proposed origami antenna.

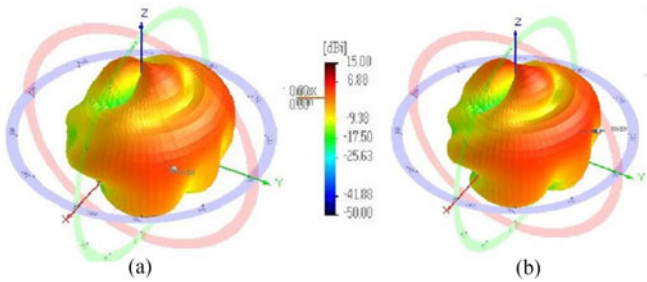

Fig. 6. Measured 3-D radiation patterns at (a) 3.5 and (b) 3.7 GHz.

the results are presented in Fig. 5. The measured and simulated 10-dB impedance bandwidths of the CP origami antenna are 70.2% (2.4–5 GHz) and 68.4% (2.4–4.9 GHz), respectively. The radiation pattern is measured using the commercial ORBIT/FR far–field measurement system in a shielded radio frequency anechoic chamber. Three-dimensional (3-D) radiation patterns are measured by rotating the fabricated antenna sample and are presented in Fig. 6(a) and (b) for the frequencies of 3.5 and 3.7 GHz, respectively. The measured and simulated ARs are presented in Fig. 7(a), and the measured 3-dB AR bandwidth

TABLE I
PERFORMANCE COMPARISON OF PROPOSED CP ANTENNA TO PREVIOUSLY PROPOSED CP ANTENNAS

	Frequency (GHz)	10 dB BW (%)	3 dB AR BW (%)	Peak Gain (dBi)	Size (mm^3)	Key Technology
[2]	0.75–1.5	25.6	16.4	3.1	$95 \times 100 \times 13.6$	Four feed network+IFA†
[3]	2–3	40	18	N/A	$150 \times 150 \times 150$	Single feed network+Parasitic Element
[4]	2.08–2.7	25	7.6	10	$120 \times 120 \times 9.3$	Single feed network+Metasurface
[5]	1.63–1.66	1.8	0.6	0.7	$69 \times 89 \times 1.57$	Two feed network+EMSIW††
This work	2.00–5.00	70.2	8.3	5.7	$270 \times 135 \times 135$ ($70 \times 70 \times 16$) †††	Two feed network+Origami

†IFA (Inverted-F antennas), ††EMSIW (Eighth-mode substrate-integrated-waveguide), †††Size after folding papers

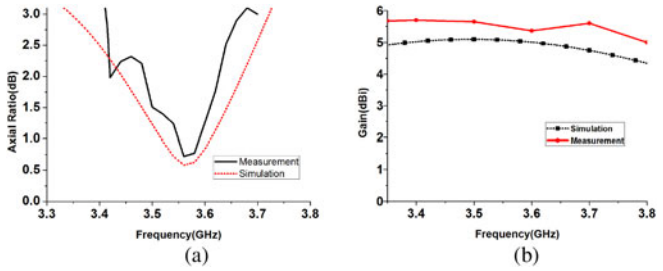

Fig. 7. Origami antenna's (a) AR as a function of frequency, and (b) LHCP gain across the 3-dB AR bandwidth.

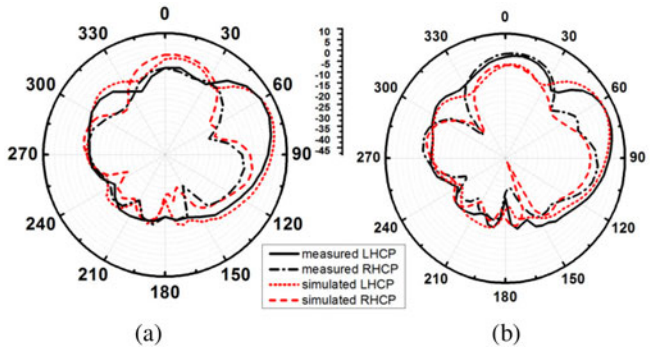

Fig. 8. Simulated and measured radiation patterns of the proposed CP origami antenna at (a) 3.5 and (b) 3.7 GHz.

is 8% (3.415–3.7 GHz). From the results obtained, it is observed that the best 3-dB AR values of the proposed antenna are directed toward $\theta = 70^\circ$ and $\varphi = 35^\circ$. The simulated and measured LHCP gain values are plotted in Fig. 7(b). The measured LHCP gain of the antenna is within the range of 5.2–5.7 dBi in the entire 3-dB AR bandwidth. Fig. 8(a) and (b) illustrates the simulated and measured radiation patterns at $\varphi = 35^\circ$, at 3.5 and 3.7 GHz, respectively. The main beam of the antenna is in the direction toward $\theta = 70^\circ$ and $\varphi = 35^\circ$ because of the position of monopole with respect to the ground plane. In the above-mentioned direction, the LHCP gain is nearly 28 dB higher than the right-hand circular polarization (RHCP) gain. The radiation pattern is not symmetric because of asymmetric geometry of the feeding lines on the *yz*- and *xz*-planes. For instance, the distance of each triangular monopole element from the origin (D_1 and D_2) is different from each other on the *yz*-plane. In addition, the feeding structure is not symmetric on the *xy*-plane. Beamwidth of the antenna along elevation and azimuth plane is 44° and 52°, respectively. As shown in Fig. 8, the sidelobe level is 11 and 6 dB lower than the main beam level at 3.5 and 3.7 GHz, respectively. The slight difference between the simulation and measurement results may be due to the folding and fabrication errors. The performance of the proposed CP antenna is compared to that of the other CP antennas in Table I. Although large size is a drawback of the proposed antenna, its size can be compact by folding papers when the antenna is carried or not used.

IV. CONCLUSION

In this letter, we presented the design of a novel origami CP antenna. We realized the fully 3-D configuration of the substrate of the antenna by folding paper in the form of an origami tetrahedron. The proposed antenna consisted of two triangular monopole elements that were perpendicular to each other. To achieve CP operation, both monopole elements were excited by a phase difference of 90°. A proof-of-concept fabricated antenna prototype featured a 10-dB impedance bandwidth of 70.2% (2.4–5 GHz), a 3-dB AR bandwidth of 8% (3.415–3.7 GHz), and a high purity of LHCP (28 dB higher than that of RHCP). Therefore, the proposed origami antenna with tilted beam can be deployed for military communications.

REFERENCES

[1] H. H. Tran, S. X. Ta, and I. Park, "Single-feed, wideband, circularly polarized, crossed bowtie dipole antenna for global navigation satellite systems," *J. Electromagn. Eng. Sci.*, vol. 14, no. 3, pp. 299–305, 2014.
[2] Q. Liu, J. Y. Shen, H. L. Liu, Y. L. Wu, M. Su, and Y. N. Liu, "Low-cost compact circularly polarized directional antenna for universal UHF RFID handheld reader applications," *IEEE Antennas Wireless Propag. Lett.*, vol. 14, pp. 1326–1329, 2015.
[3] J. Fouany, M. Thevenot, C. Menudier, T. Monediere, and A. Thomas, "Circularly polarized directive antenna with parasitic elements for wide band applications," in *Proc. 13th Mediterr. Microw. Symp.*, 2013, pp. 1–4.
[4] H. L. Zhu, S. W. Cheung, K. L. Chung, and T. I. Yuk, "Linear-to-circular polarization conversion using metasurface," *IEEE Trans. Antennas Propag.*, vol. 61, no. 9, pp. 4615–4623, Sep. 2013.
[5] K. Kim and S. Lim, "Miniaturized circular polarized TE-mode substrate-integrated-waveguide antenna," *IEEE Antennas Wireless Propag. Lett.*, vol. 13, pp. 658–661, 2014.
[6] X. Liu, S. V. Georgakopoulos, and M. Tentzeris, "A novel mode and frequency reconfigurable origami quadrifilar helical antenna," in *Proc. IEEE 16th Annu. Wireless Microw. Technol. Conf.*, Cocoa Beach, FL, USA, 2015, pp. 1–3.
[7] X. Liu, S. Yao, B. S. Cook, M. M. Tentzeris, and S. V. Georgakopoulos, "An origami reconfigurable axial-mode bifilar helical antenna," *IEEE Trans. Antennas Propag.* vol. 63, no. 12, pp. 5897–5903, Dec. 2015.
[8] S. W. Lee and Y. Sung, "Polarization diversity patch antenna with reconfigurable feeding network," *J. Electromagn. Eng. Sci.*, vol. 15, no. 2, pp. 115–119, 2015.
[9] Y. Jin, J. P. Tak, and J. H. Choi, "Quadruple band-notched trapezoid UWB antenna with reduced gains in notch bands," *J. Electromagn. Eng. Sci.*, vol. 16, no. 1, pp. 35–43, 2016.
[10] J. S. Park, J. B. Ko, H. K. Kwon, B. S. Kang, B. Park, and D. Kim, "A tilted combined beam antenna for 5G communications using a 28-GHz band," *IEEE Antennas Wireless Propag. Lett.*, vol. 15, pp. 1685–1688, 2016.